

Transition from metallic to tunneling-type conductance in metal-metal and normal-metal–superconductor point contacts

H. Srikanth and A. K. Raychaudhuri

Department of Physics, Indian Institute of Science, Bangalore 560012, India

(Received 14 April 1992; revised manuscript received 30 July 1992)

We have investigated the microshort-to-tunneling crossover in normal-normal ($N-N$) and normal-metal–superconductor ($N-S$) point-contact junctions at 4.2 K as the junction conductance (G_0) is varied. The microshort (or “metallic”) point contact with the dynamic conductance $G(V)$ having a negative derivative with respect to bias V (i.e., $\partial G/\partial V < 0$) changes over to a tunneling-type junction with $\partial G/\partial V > 0$ when $G_0 \approx 3-5$ mS. We show that this is the region where the contact radius a is a few times k_F^{-1} (k_F is the Fermi wave vector) and the crossover in the sign of $\partial G/\partial V$ occurs due to electron confinement in a length scale comparable to k_F^{-1} . The effect of confinement is to make the electrons crossing the constriction evanescent in nature as the junction size is reduced progressively and the energy for lateral confinement becomes comparable to E_F . We argue that in this extreme ballistic regime, the classical Sharvin approach breaks down as quantum effects due to electron confinement takes over. This happens much before “single-atom” contact is reached which signals the onset of vacuum tunneling. As a further test of the electron confinement effects in point contacts, we investigated clean $N-S$ microshorts showing near-ideal Andreev reflection. We find that in $N-S$ junctions, the Andreev reflection (which is a manifestation of superconductivity) gradually vanishes when the contact radius $a \approx 0.1\xi$ (ξ is the coherence length) and the energy cost of electron confinement is larger than the superconducting energy gap Δ .

I. INTRODUCTION

The transition from a microshort to a tunneling region in a point contact is a topic of current interest. With the advent of the scanning tunneling microscope (STM),¹ a number of experimental studies has been reported in this area.² When a sharply etched metal tip is placed on a metal surface ($N-N$ junction), there are two limiting regions. When the tip is in close contact with the surface, we get a metallic point contact (microshort). This region has been used extensively in the past in studies of spectroscopy of elementary excitations in solids commonly referred to as point-contact spectroscopy³ (PCS). PCS is done in the region of ballistic transport where the constriction or the contact size given by radius a is smaller than the elastic mean free path of the electron, l_e . The other limit is the region of vacuum tunneling, when the tip is not in mechanical contact with the substrate and is positioned at a certain distance away from it (≈ 10 Å). In a ballistic metallic point contact, the conductance of the junction is typically $> 10^{-2}$ S. In the case of a tunneling-type junction, as encountered in a STM, the junction conductance is typically $< 10^{-7}$ S. In between these two limits lies the region of transition. In this paper, we report on certain characteristics of this transition as revealed through dynamic-conductance studies [dI/dV]- V] of point-contact junctions at low temperatures ($T=4.2$ K).

Point-contact spectroscopy using metallic point contacts is done in the ballistic region when $l_e > a$. This is usually called the “Sharvin limit.”⁴ In the other extreme ($a > l_e$) one is in the classical, “Maxwell limit.”³ The resistance of a point contact as a function of the Knudsen ratio ($K \equiv l_e/a$) is given by³

$$R_0 = (4\rho l_e / 3\pi a^2) \{ 1 + (3\pi/8)\Gamma(K)(a/l_e) \}, \quad (1)$$

where ρ is the bulk resistivity of the material and $\Gamma(K)$ is a smooth function of K such that, for the Sharvin limit ($K \gg 1$), $\Gamma(K) \rightarrow 0.694$ and

$$R_0 = R_{\text{Sharvin}} = 4\rho l_e / 3\pi a^2. \quad (2)$$

In the Maxwell limit, $K \rightarrow 0$ and $\Gamma(K) \rightarrow 1$, giving

$$R_0 = R_{\text{Maxwell}} = \rho / 2a. \quad (3)$$

In the Sharvin limit, the presence of ρl_e ensures a simple relation in terms of the fundamental unit of resistance (\hbar/e^2):

$$R_{\text{Sharvin}} = 4(\hbar/e^2)(k_F a)^{-2}. \quad (4)$$

The advantage of writing the Sharvin formula in the form of Eq. (4) is that the constriction resistance can be easily converted into a contact radius a which is measured in the units of k_F^{-1} , a natural length scale for an electron.

In terms of conductance $G_S (= 1/R_S)$ the Sharvin formula,

$$G_S = \frac{1}{4}(e^2/\hbar)(k_F a)^2, \quad (5)$$

becomes a measure of the number of channels if we use the Landauer relation⁵ of conduction through a single (barrierless) channel:

$$G_c = e^2 / \pi \hbar. \quad (6)$$

The Sharvin conductance G_S (which is actually valid for a zero-area contact, i.e., $a/l_e \rightarrow 0$) has no energy scale in the sense that in this limit, G_S should become indepen-

dent of the bias voltage V applied across the junction. The bias-voltage dependence of the differential point-contact conductance ($G = dI/dV$) arises from the back-scattered electrons at the point contact.^{3,6} In general, for metallic point contacts, G is maximum at $V=0$ and G decreases with increasing voltage [see Fig. 1(a)]. (The presence of magnetic excitations or superconductivity often introduces additional features on this background; however, for this discussion, we neglect these features.) As the voltage dependence of G gives a measure of $\tau^{-1}(eV)$, where τ is the electron scattering time in the bulk, the decrease of G with V is generally believed to arise from lattice phonons. It is expected that, as a decreases (which implies fewer channels for conduction in the Landauer formalism), the voltage dependence of G should vanish because, in the classical Sharvin relation, the conductance has no voltage dependence. This point, however, has not been explicitly pointed out by experiments in this field. In the present investigation we address this question. It is important to realize that the Sharvin relation is a classical relation which is valid in the limit $a/l_e \rightarrow 0$. However, a has a lower limit for the junction to behave classically. We will argue that for junctions which are so small that $a \sim k_F^{-1}$, the wave nature of the electron becomes important and the Sharvin relation ceases to be meaningful.

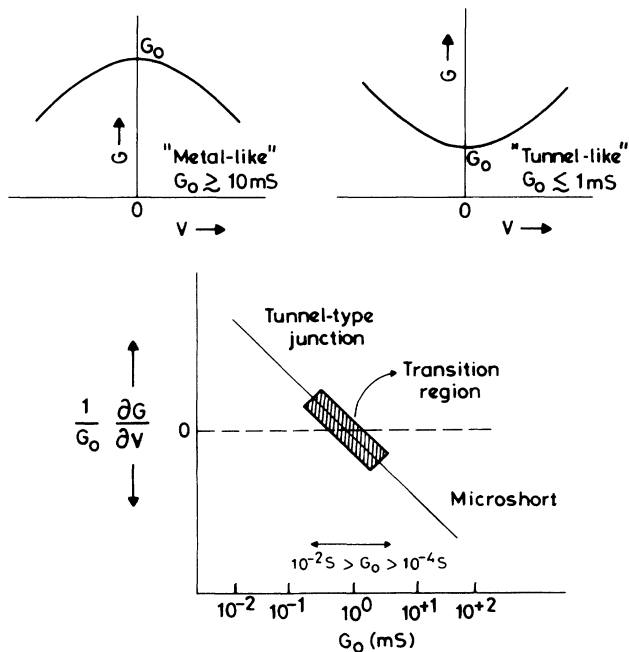


FIG. 1. (a) A schematic representation of the variation of the dynamic conductance (dI/dV) with the bias voltage (V) for a typical microshort and tunnel junction. G_0 are the typical zero-bias conductance values for which such contrasting behavior is seen. (b) Schematic showing the crossover from microshort to tunneling regimes as seen through change of sign of $\partial G/\partial V$. The hatched portion represents the typical conductance range over which the transition could occur. Note that $\partial G/\partial V=0$ indicates the ideal Sharvin conductance, in which case dI/dV is independent of the applied bias.

In the tunneling regime, G always increases with V . (We are, for the time being, excluding features in the tunneling curves which may arise from strong energy dependence in the density of states as in a superconductor.) In a typical $N-I-N$ junction, $G \propto G_0(1 + \beta V^2)$ and the parabolic dependence is a measure of the tunneling barrier strength.⁷ In a STM, one has a tunnel junction of extremely small size and capacitance $C (\approx 10^{-18} - 10^{-19} \text{ F})$ so that single-electron-tunneling phenomena become important, leading to a Coulomb blockade. This has been seen experimentally by various authors.⁸ In a recent experiment, using crossed-wire geometry and adsorbed helium as the insulating barrier, it was shown that the dip in conductance G due to Coulomb blockade vanishes when the junction conductance is more than $G_0 \approx 1.5 \times 10^{-4} \text{ S}$, which would imply a conductance $\approx e^2/\hbar$.⁹ This shows that, for a junction with sizes larger than a single or few conduction channels, the single-electron charging effects as revealed through $G-V$ curves tend to vanish. Whichever may be the case, when the junction conductance $G_0 < 1 \text{ mS}$, one observes that G increases with increasing bias V . The transition from ballistic microcontact (for junctions with $G_0 > 10^{-2} \text{ S}$) to tunneling-type junctions (with $G_0 < 10^{-4} \text{ S}$) can then be seen in $G-V$ curves. At certain conductance $10^{-2} > G_0 > 10^{-4} \text{ S}$, the slope $\partial G/\partial V$ of the $G-V$ curve should change from negative in a microshort junction to positive in a tunnel-type junction. We illustrate this schematically in Fig. 1(b).

Another important observation in a microshort-to-tunneling transition on clean junctions was made using a STM working in ultrahigh vacuum.² In this experiment, the junction conductance was studied as a function of tip-sample separation. It was observed that for junctions with conductances $< 10^{-7} \text{ S}$, the current depends exponentially on the distance indicating vacuum tunneling. However, for junctions with conductance $\approx 10^{-4} \text{ S}$, there is a sharp jump in the conductance and after that the current varies rather slowly with the tip displacement, showing the onset of mechanical contact. This experimental observation triggered a number of theoretical investigations and the conductance jump occurring for the junction conductance $\approx 10^{-4} \text{ S}$ has been interpreted as the onset of "single-atom" contact.¹⁰ This conductance is close to G_c [see Eq. (5)], the single-channel Landauer conductance.⁵ However, no $G-V$ curves were reported for these junctions close to the microshort-tunneling transition. The above discussion raises the question whether the $G-V$ curve changes from a metallic ($\partial G/\partial V < 0$) to tunneling ($\partial G/\partial V > 0$) type around the same region of junction conductance where one observes single-atom contact.

In this paper we address this particular issue related to the change in the sign of $\partial G/\partial V$. We show that the change in the sign of $\partial G/\partial V$ occurs at a much higher junction conductance ($\approx 3 \text{ mS}$) and we suggest that this change occurs due to electron confinement in a narrow channel before single-atom contact is attained.

As a test of the effects of electron confinement we also extend this experiment to normal-metal-superconductor ($N-S$) point contacts. In a high-conductance $N-S$ point contact, one sees an Andreev reflection for $|V| < \Delta$ (su-

perconducting gap).^{11,12} We find that as the junction conductance is decreased and the contact radius a becomes a certain fraction of the coherence length ξ ($a \simeq 0.1\xi$), the signature of the Andreev reflection vanishes and eventually the contact behaves like a normal junction, which, like any other N - N junction, shows a change of sign of $\partial G/\partial V$ (from negative to positive) at an even lower junction conductance. The absence of an Andreev reflection for junctions with $a \simeq \xi/10$ is also suggested as due to electron confinement.

The concept we would like to stress is that, in the transition region, the contact size becomes so small that quantum effects arising from electron confinement become important. The experiments reported in this paper are attempts to bring out these issues.

The following part of the paper is divided into three sections. In Sec. II, we briefly describe our experimental arrangement. The results are presented in Sec. III, followed by a discussion in Sec. IV.

II. EXPERIMENT

The experiments were carried out at 4.2 K by dipping the junctions in liquid helium. The junction conductance ($G = dI/dV$) was measured either by a dc method (using a programmable current source and voltmeter) and subsequent numerical differentiation of the I - V data or by an ac method (using a modulation technique at $f \simeq 327$ Hz and a lock-in amplifier). The details of the cryostat and the electronics are given in a separate publication.¹³

The mechanical system for the positioning of the tip on the substrate consists of a differential screw (coarse positioner) and a PZT tube (fine positioner). The differential screw can be operated from room temperature by a drive rod. This enables us to make the junction after the sample is immersed in liquid helium.

The tips used in the experiments (Au or Pt) were made by electrochemical etching and the substrates used (Pt, Nb, and Pb) were mechanically cleaned prior to loading into the cryostat. Usually, before cooling down the cryostat, the sample region is purged with helium gas for some time at room temperature and then the cryostat is cooled by dipping in liquid helium. The tip is first made to touch the substrate and a low-resistance junction is formed. After that the tip is slowly retracted (or the contact area reduced) by releasing the contact pressure to obtain higher-resistance junctions. The formation of the low-resistance junction ensures that at least in the area of contact there is no appreciable barrier or adsorbate. From the reproducibility of the data as well as near perfect observation of the Andreev reflection in N - S contacts, we think this “*in situ*” (brute force) cleaning gives us a clean barrierless junction. The process makes the tip relatively blunt and one cannot use it for usual STM imaging. However, for our work this is not important. We get a measure of the contact size from Eq. (1), though the exact geometrical form will be an uncertainty. For ease of reference we will use the notation Au(tip):Pt to mean that this is a junction made from a Au tip and Pt substrate. We also use the convention that positive bias implies that the tip is biased positively with respect to the

substrate. We have studied two N - N junctions [namely, Pt(tip):Pt and Au(tip):Pt] and three N - S junctions [namely, Pt(tip):Nb, Au(tip):Nb, and Au(tip):Pb]. In the following section we present the results.

III. RESULTS

A. Normal-metal–normal-metal (N - N) junction

In Figs. 2 and 3 we show the G - V curves for two N - N contacts. In both figures, the conductances are normalized with respect to the zero-bias conductance G_0 . (The values of G_0 for the junctions are shown in the figures.) We can see that in both the junctions [Pt(tip):Pt in Fig. 2 and Au(tip):Pt in Fig. 3] for G_0 more than a few mS, $\partial G/\partial V$ is negative and $|(1/G_0)(\partial G/\partial V)|$ increases as G_0 increases. This is the region generally used for *point contact spectroscopy*.³ For junctions with $G_0 \simeq 0.01$ S, from Eq. (5) we find that $ak_F \simeq 7.2$. For Pt, $k_F \simeq 1.2 \times 10^{-8}$ cm⁻¹, which implies that $a \simeq 6$ Å. The mean free path of electrons in these materials, at 4.2 K, $l_e \simeq 1$ μm. Thus, junctions with $G_0 \simeq 0.01$ S are clearly in the ballistic regime with very high Knudsen number. For both junctions, we find that $\partial G/\partial V$ changes sign when $G_0 \simeq 3$ –5 mS. To see clearly the change of sign in Fig. 4, we have plotted $(1/G_0)(\partial G/\partial V)$ as a function of G_0 . For Au(tip):Pt, $\partial G/\partial V \simeq 0$ for $G_0 \simeq 5$ mS. This would imply $ak_F \simeq 5.14$ and $a = 4.3$ Å. For Pt(tip):Pt this occurs for $G_0 \simeq 3$ mS with $ak_F \simeq 4.0$ and $a \simeq 3.3$ Å. This is comparable to the lattice spacing in Au and Pt (4.08 Å for Au and 3.92 Å for Pt). Thus, the change in the sign of $\partial G/\partial V$ comes when the contact radius is comparable to the lattice spacing of atoms in the bulk material. This size is larger than the size of an atom. Thus, the crossover from metallic- to tunneling-type contact as revealed through the slope of G - V curves occurs before “single-

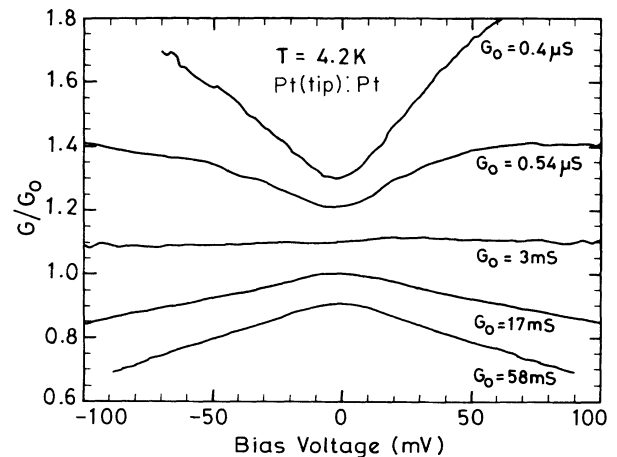


FIG. 2. The microshort-tunneling transition curves for variable conductance Pt(Tip):Pt point-contact junctions at 4.2 K. The curves have been normalized with respect to the zero-bias conductance G_0 and relatively shifted for clarity. The corresponding G_0 values are marked alongside the curves. Note the almost flat G - V data for $G_0 = 3$ mS.

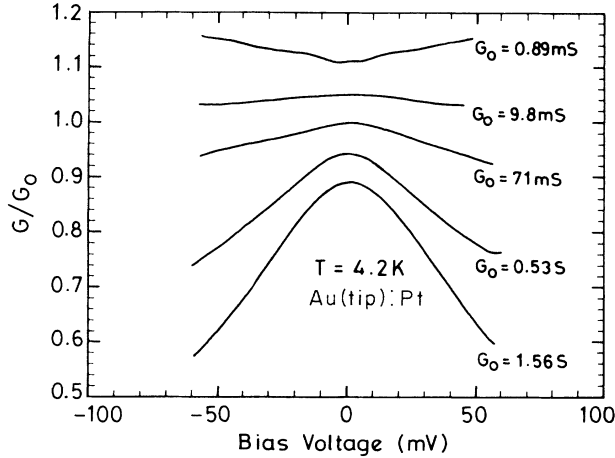


FIG. 3. The evolution of conductance characteristics in Au(tip):Pt point-contact junctions at 4.2 K. The data have been normalized with respect to the zero-bias conductance G_0 and relatively shifted. The G_0 values varying over 4 orders in magnitude are indicated in the graph.

atom" contact is attained. Beyond "single-atom" contact, one sees vacuum tunneling. This is an important observation made in these N - N point contacts in the present work. It must be pointed out that such observations in studies with point contacts have been made before.¹⁴ However, it was never explicitly discussed in the context of a microshort-to-tunneling transition. This observation then leads to the question as to why $\partial G/\partial V$ should change sign when the electron is confined in the region of "few-atom" contacts. We discuss this later on in Sec. IV.

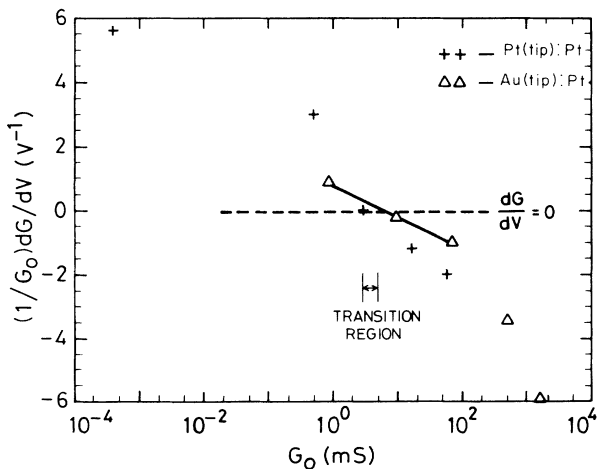


FIG. 4. Plot showing $(1/G_0)\partial G/\partial V$ vs G_0 for the different sets of curves shown in Figs. 2 and 3 for Pt(tip):Pt and Au(tip):Pt point-contact junctions. The microshort-tunneling transition indicated by the change of sign of $(1/G_0)\partial G/\partial V$ from negative to positive occurs within an order of magnitude in G_0 for both cases. Note: The solid and dashed lines drawn in the graph are just guides for the eye.

B. Normal-metal-superconductor (N - S) junction

In the case of N - S point contacts, in addition to the contact size a and the Fermi wave vector k_F , we have another length scale (namely, the coherence length ξ) and an energy scale (the superconducting energy gap Δ). The coherence length $\xi [=(\hbar v_F/\pi\Delta)]$ being much larger than the lattice spacing, one would expect that much before "few-atom" contacts are reached (signaled by change in sign of $\partial G/\partial V$ as in the N - N case) one should see effects arising out of electron confinement in the superconducting properties of N - S point contacts. The motivation for doing these experiments with N - S point contacts is to investigate these aspects.

In Figs. 5–7 we present our data on Pt(tip):Nb, Au(tip):Pb, and Au(tip):Nb junctions taken at 4.2 K. In Fig. 5 [Pt(tip):Nb], we show data taken close to zero bias. In these point contacts, we find the following behavior close to zero bias $|V| < 4$ meV: We first take the example of the Pt(tip):Nb junction. For the junction with the highest conductance ($G_n \approx 2.7$ S), we find a pronounced peak around zero bias which goes down rather sharply at $|V| \approx 1$ meV. G then shows a small dip at $|V| \approx 1.2$ meV and for $|V| > 2$ meV, G settles to a much weaker variation with V similar to those in N - N junctions of high conductance with $\partial G/\partial V < 0$. The value of V where the dip occurs in G matches closely with the superconducting energy gap of Nb (Δ_{Nb}) at 4.2 K. The excess conductance at $V=0$ and its sharp fall as $|V| \rightarrow \Delta_{\text{Nb}}$ is interpreted as arising due to Andreev reflection.¹² There are quite a few reports of observations of the Andreev reflection in clean N - S contacts, including those on high- T_c superconductors.¹⁵ For a clean, ideal, N - S point contact showing an

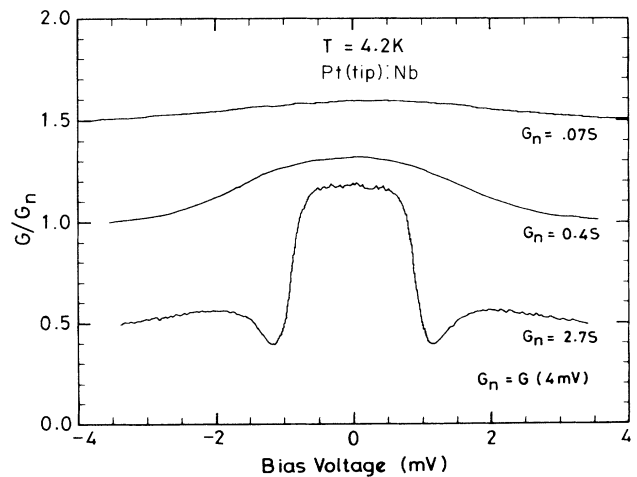


FIG. 5. A set of normalized conductance curves for Pt(tip):Nb point-contact junctions at 4.2 K showing the gradual disappearance of the excess conductance at zero bias. The conductance at 4 mV is taken as the normal-state conductance and curves are relatively shifted for clarity. Note that the ratio G_0/G_n is 2 (in the lowermost curve with $G_n = 2.7$ S), which is the signature of the Andreev reflection in barrierless N - S interface. The symmetric dips seen in the same curve occur at $|V| = 1.2$ mV, which is the superconducting gap value of Nb.

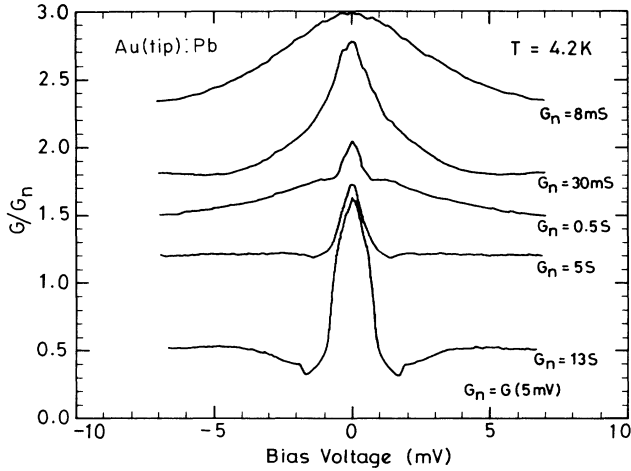


FIG. 6. The normalized conductance curves showing the gradual smearing of the Andreev reflection signal in Au(tip):Pb point-contact junctions at 4.2 K as the junction conductance is lowered. The curves are normalized with respect to $G(5 \text{ mV})$, which is taken as the normal-state conductance G_n and relatively shifted for clarity. The ratio G_0/G_n for the lowermost curve which is in excess of 2 could be due to proximity effects in addition to the Andreev reflection.

Andreev reflection, the ratio $G_0/G(|V| > \Delta) \rightarrow 2$.¹² For the Pt(Tip):Nb contact we find $G_0/G(4 \text{ mV}) \approx 1.6$, indicating that an almost barrierless N - S point contact can be formed in these experiments for junctions with relatively high conductance (typically $> 1 \text{ S}$). In Fig. 6, we make a similar observation for Au(tip):Pb junctions ($\Delta_{\text{Pb}} \approx 1.4 \text{ meV}$). In this case one also sees a large excess conductance near zero bias. In Au(tip):Pb, for the

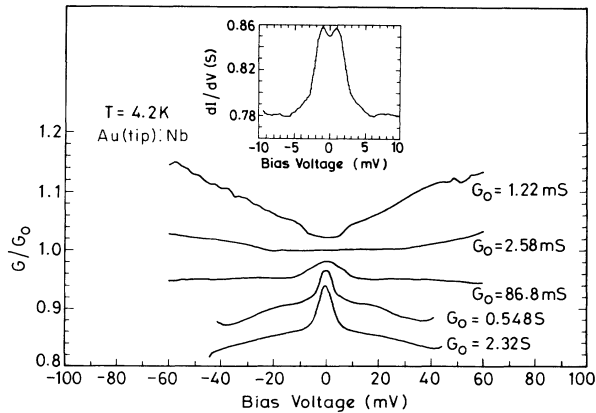


FIG. 7. Microshort-tunneling transition curves for a Au(tip):Nb point-contact junction at 4.2 K. For high-conductance junctions, the conductance peak at zero bias in addition to the overall decreasing background (G - V) is due to the superconductivity of Nb. The curves are normalized with respect to zero-bias conductance G_0 and relatively shifted. The inset shows the (dI/dV) - V curve over a low voltage range in a high-conductance junction. The small G_0/G_n ratio and the dip at zero bias is due to presence of a finite barrier at the Au(tip):Nb interface (most likely due to surface oxide on Nb).

highest conductance junction ($G_n \approx 13 \text{ S}$), the ratio $\rightarrow 2$ and it decreases to around 1.6 when $G_n \approx 5 \text{ S}$. For Au(tip):Nb N - S point contacts we observe qualitatively similar behavior as in other junctions but there are certain differences. First of all, even in the highest conductance junction ($G_0 \approx 2 \text{ S}$), the magnitude of the zero-bias peak $G_0/G(|V| > \Delta) \approx 1.1$, which is much lower than those observed in Pt(tip):Nb and Au(tip):Pb junctions. Second, even the junction with the highest conductance shows the existence of a small but finite barrier and this can be seen as a split peak in the conductance near zero bias as shown in the inset of Fig. 7. These features are in agreement with Blonder-Tinkham-Klapwijk (BTK) theory for N - S point contacts. [In BTK theory, the assumed barrier at N - S junction is a δ -function barrier and the junction is characterized by a dimensionless barrier constant Z . As Z increases, a dip develops in the conductance curve at $V=0$ and gradually peaks appear at $|V| = \Delta$. For a strong barrier (i.e., large Z) the G - V curve looks similar of that of a tunnel junction with a grown barrier.] The gap that is estimated from the split peak is $\approx 1 \text{ meV}$. This is less than that obtainable for bulk Nb. We suspect that in this case the Au tip has not succeeded in piercing through the oxide on Nb completely. At this point we digress a little to point out certain interesting and unexplained aspects of the observed G - V curves in clean N - S contacts. In Fig. 8, we have shown the experimental data for Pt(tip):Nb and Au(tip):Pb junctions showing an Andreev reflection. In the same graph, with a dotted line we show the expected curve from BTK theory. We find that near the gap a dip occurs (at $|V| \approx \Delta$ in normalized G - V curves). This has been observed even in high- T_c materials.¹⁵

The feature of N - S point contact which is of importance to us is the qualitative difference of the conductances near zero bias ($|V| < \Delta$) for high-conductance N - S and N - N contacts. In the N - S contacts, $G(|V| > \Delta)$ decreases with increasing V and this is very similar to that in N - N contacts. However, the superconducting feature of the point contact is revealed through the Andreev reflection or an “excess conductance” near zero bias for $|V| < \Delta$.

As the junction conductance of the contacts is reduced, we find that the features associated with the Andreev reflection become less pronounced. The conductance at zero bias $G_0/G(|V| > \Delta)$ gradually decreases from the ideal value 2, the central peak broadens considerably, and the small dips in G at $|V| \approx \Delta$ tend to vanish. For all these junctions, any trace of the Andreev reflection vanishes for $G_0 < 1 \text{ S}$, though a broad background showing a maximum at zero bias persists up to $G_0 \approx 0.1 \text{ S}$ (see Figs. 5–7). For $G_0 < 0.1 \text{ S}$, the G - V curves are rather similar to those obtained in N - N junctions and, finally, the $\partial G/\partial V$ changes sign for $G_0 \approx 3$ – 5 mS as in N - N junctions. This can be clearly seen in Fig. 6. The value of $G_0 \approx 1 \text{ S}$ where the distinct Andreev reflection disappears corresponds to $ak_F \approx 70$. For Nb this would mean $a \approx 60 \text{ \AA}$, which is much smaller than ξ ($\approx 1000 \text{ \AA}$ for Nb) but larger than “few-atom” contacts where $\partial G/\partial V$ changes sign. We will discuss this absence of the Andreev

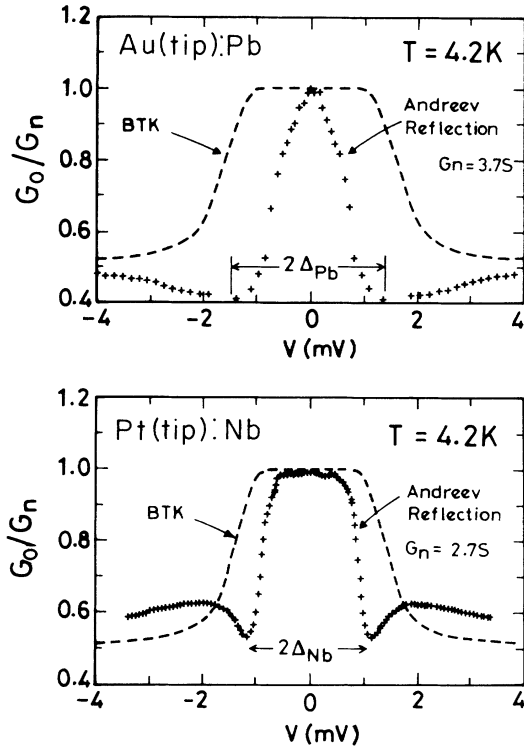


FIG. 8. The experimentally observed conductance curves for Au(tip):Pb and Pt(tip):Nb N - S point-contact junctions at 4.2 K (+ + +) along with the fits generated by BTK theory (---) assuming an ideal barrierless ($Z=0$) N - S interface and taking the superconducting gaps of Pb and Nb to be 1.5 and 1.3 meV, respectively. The data are normalized with respect to the zero-bias conductance G_0 . Note that the conductance falls to its normal-state value at a much faster rate than predicted by the BTK model and symmetric dips occurs at the gap voltages of Pb and Nb.

reflection for junctions with a length scale shorter than ξ further in Sec. IV. We note the observation of a gradual change in the N - S point-contact characteristics as a function of junction conductance.

The experiments on N - N and N - S point contacts very clearly demonstrate the effect of electron confinement as one goes from a large size contact ($a \gg k_F^{-1}$) to an atomic ($a \approx k_F^{-1}$) size contact. In the following section, we would like to discuss our experimental results with an attempt to provide a physical explanation for these effects. Another possibility exists to explain the general behavior of a change in sign of $\partial G/\partial V$ from negative to positive going through a region where $\partial G/\partial V=0$ as one goes from a metallic- to a tunneling-type junction. This is the simple assumption of the point contact as a parallel combination of microshorts and tunnel junctions. A flat $G(V)$ curve can be obtained just due to the two competing effects canceling each other. However, the fact that the crossover takes place in a specified conductance range 3–5 mS for a variety of junctions with different materials makes this scenario less probable. Moreover, in the case of N - S point contacts, the Andreev reflection peak in dI/dV should gradually split up into two peaks at $\pm \Delta$

with a dip at zero bias as the tunneling starts to dominate over the microshorts. Our experimental data shown in Figs. 5 and 6 indicate a broadening of the zero-bias peak as the junction conductance decreases. Based on our observations, we believe that confinement effects due to size constraint could be most important, which determines the nature of $G(V)$ curves around the crossover region.

At this point we refer to some earlier experiments which also investigated the issue of a metallic-to-tunneling transition in S - N or S - N - S point contacts, including an experiment on the Cu(tip):Nb system.¹⁶ Though the data obtained by us have some similarity with the Cu(tip):Nb data, they differ significantly in three aspects. First, in the Cu(tip):Nb data, a barrierless ($Z=0$) N - S contact was never seen and it showed effects which may arise from a surface oxide barrier. Second, the issue of electron confinement was never raised and their proposed explanation is different from that offered by us. Third, in the Cu(tip):Nb experiment, no attempt was made to look into low-conductance junctions ($G_0 < 1$ mS), where one sees the manifestation of microshort-tunneling transition in N - S contacts.

Another experiment was done on superconductor–heavily-doped-semiconductor lithographically fabricated microbridges.¹⁷ In this experiment, the microbridge size (0.5–1 μm) was kept fixed and the microbridge (planar) had an S - N - S structure. The authors observed a transition from “Andreev-type” ($Z=0$) to “tunneling-type” ($Z \gg 1$) conductance curves as the doping level of the normal-metal region was progressively reduced. However, the conductance curves in the transition region showing a smooth evolution from one type to the other has not been shown. In this experiment, the junction size was kept fixed and the barrier Z was tuned by changing the doping level. Since the constriction size ($\geq 0.5 \mu\text{m}$) was large, the electron confinement aspect is not of importance. Similar observations on the microshort-to-tunneling transition has been made by us in Au(tip):YBa₂Cu₃O_{7- δ} (single crystal) point-contact junctions.¹⁵

IV. DISCUSSION

The first question we would like to look into is the “critical” contact size where $\partial G/\partial V$ changes sign. Our approach to this problem will be to use simple concepts to settle the length scales in the problem. For simplicity we assume the point-contact region to be like a narrow constriction of radius a and length $> 2a$. This is shown in Fig. 9(a). For the conduction through the contact to be metallic, one should have a propagating wave. If k_{\parallel} is the momentum of the electrons in the direction of propagation through the contact, k_{\parallel} should be real for a metallic contact. Since there is confinement (on a scale $\approx 2a$) in the lateral direction, the transverse momentum k_t has a lower bound given by $\pi/2a$ so that the minimum energy of the transverse electron $(E_t)_{\min} \approx (\hbar^2 \pi^2 / 4ma^2)$. As $T \rightarrow 0$, the conduction is due to states with energy $E \approx E_F$. (For bias $|V| < 100$ mV, $e|V| \ll E_F$). Since E_t can have minimum value of $\hbar^2 \pi^2 / 4ma^2$ due to confinement, this imposes a maximum on

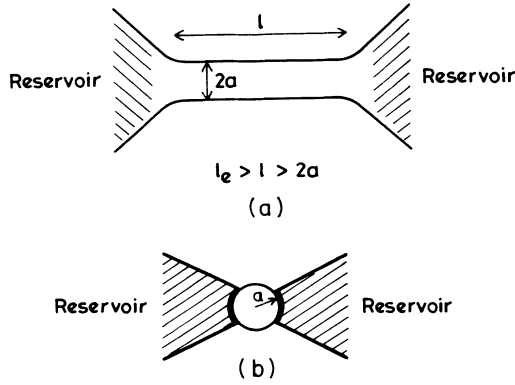


FIG. 9. Two schematic views of the point contact as a micro-constriction connecting bulk reservoirs on either side. The point contact can be treated as a narrow cylindrical channel of length l and radius a as shown in (a), where l_e is the elastic mean free path of the electron. (b) illustrates the Kubo formalism where the point contact is treated as a small spherical particle of radius a .

$E_{\parallel} = E_F - \hbar^2 \pi^2 / 4ma^2$. When the constriction is so small that $(E_{\parallel})_{\min} \simeq E_F$, the only possible real value is $k_{\parallel} = 0$. Thus, for extremely small a , k_{\parallel} ceases to be real. Thus, the minimum constriction size which allows a propagating wave along the constriction is given by the condition $\hbar^2 \pi^2 / 4ma^2 \leq E_F$ or $ak_F \geq 2$.

One obtains a similar result if one considers the point-contact region as a small particle of radius a . In this picture the small particle of radius a is connected to large reservoirs on two sides. This is shown in Fig. 9(b). For a grain of radius a , we obtain from the Kubo formula¹⁸ the electron-energy-level separation

$$\delta = E_F / \pi a^3 n, \quad (7)$$

where n is the electron density. Using $n = k_F^3 / 3\pi^2$, we obtain

$$\delta / E_F = 3\pi / ak_F^3. \quad (8)$$

If the spherical contact region of size a has to act as a metallic contact between the two reservoirs, then $\delta < E_F$. Otherwise the region will act as an insulator (for $T \rightarrow 0$). Therefore, for a metallic point contact, one must have $ak_F > (3\pi)^{1/3} \simeq 2.1$, which is the same result as obtained before. (This relation is similar to the Ioffe-Regel criterion for propagation of electron waves in a solid.¹⁹ In a solid the microscopic length is determined by the electron mean free path.) For junctions with $G_0 \simeq 3-5$ mS, where the change in sign of $\partial G / \partial V$ occurs, we found that $ak_F \simeq 4$. This is close to what is estimated by simple considerations which do not take into account details of the contact. The above discussion implies that $\partial G / \partial V$ starts changing sign when an appreciable part of the electrons crossing the junction are of evanescent type, with k_{\parallel} becoming imaginary. For ballistic propagation, we need a junction with high Knudsen number $l_e / a \gg 1$ and the junction conductance approaches the voltage-

independent Sharvin value. However, there is a break of the classical Sharvin relation at this point as the electron is being confined within a size comparable to k_F . For these point contacts, quantum size effects are bound to show up and our experiment therefore shows the critical limit of the classical ballistic Sharvin conductance. In point-contact spectroscopy using metallic contacts ($\partial G / \partial V < 0$) one has to stay away from this regime to avoid quantum confinement effects.

The total current I through such a small point-contact junction can be broken down into parts, $I = I_t + I_B$, where I_t represents a current carried by the evanescent electrons and I_B , that carried by the propagating ballistic electrons. This breakup of the current is a division in terms of electron energy which will determine if k_{\parallel} is real or imaginary. At this point we would like to mention that I_B , which we take here as a pure ballistic current, can have additional higher-order contributions due to backscattering of the ballistically propagating electrons into the contact area. This would lead to an effective decrease in the junction conduction as a function of bias voltage. Point-contact spectroscopy is done in this regime and a discussion of the negative $\partial G / \partial V$ in ballistic non-Sharvin metallic contacts can be found in the literature.^{3,6} Here we consider the case close to the crossover (i.e., $\partial G / \partial V = 0$ to positive) where confinement effects are important.

In the limit $l_e \gg a \simeq k_F^{-1}$, the current I_B , which is due to ballistic electrons, is given by $I_B = G_S V$. Since the classical Sharvin conductance G_S has no voltage dependence, this term contributes a constant term to the total conductance $G (= dI / dV)$. The voltage dependence of G therefore comes predominantly from the term dI_t / dV . The current I_t , being due to evanescent electrons, is like a tunneling current and $dI_t / dV > 0$. In this case the barrier is not a physical barrier (as in vacuum tunneling) and is due to confinement. (If the energy $E > E_F$, then there will be an effective barrier $E - E_F$.) For $G_0 < 0.1$ mS, when the one-atom contact is broken, one enters the vacuum tunneling regime with a physical barrier. It therefore appears that the electron confinement in the tip contact area will determine the energy scale which will split the electrons crossing the junction into propagating type and evanescent types. This will show up as a gradual change in sign of $\partial G / \partial V$ with the transition occurring when $ak_F \simeq 2-4$.

This simple idea of electron confinement has been developed into a more rigorous theory of quantum point contacts (QPC) where the steplike jumps in the junction conductance in narrow channel metal-oxide-semiconductor field-effect transistors (MOSFET's) as a function of channel width (which can be controlled by an applied voltage) were investigated.²⁰ In these junctions, the steplike jumps in the conductance arise due to discrete splitting of energy levels of the electrons in the confined dimension of the channel. These theories were also applied in STM investigations of ballistic-to-tunneling transitions where one sees effect of single-atom contact.¹⁰ It will be of interest to see how these theories and models can be used to evaluate the voltage depen-

dence of G as one approaches junctions of few atomic dimensions starting from the metallic side where classical Sharvin formulation is valid. Our results suggest that the effect of lateral confinement below a certain size of the point contact is to introduce evanescent character to the electrons crossing the junction.

As a check of this picture of electron confinement we now turn our attention to N - S point contacts. Here, we have an additional energy scale (Δ), the superconducting gap or length scale (ξ), the coherence length. We confine our attention to the Andreev reflection which is a characteristic of the superconducting nature of the junction. In this case, the electrons in question (i.e., those taking part in the Andreev reflection) have an energy confined within $\pm\Delta$ of E_F . If the energy due to electron confinement is larger than Δ , then these electrons will behave as normal electrons. This situation is similar to that of superconductivity in small particles. Using the definition of $\xi = \hbar v_F / \pi \Delta$, we have

$$\Delta / E_F \simeq (2/\pi)(\xi k_F)^{-1}. \quad (9)$$

Rewriting Δ in this form sets the scale of ξ in terms of k_F^{-1} which we are using as a natural length scale. In N - N junctions we see the effects of confinement when $a \simeq k_F^{-1}$. In N - S junctions, since the length scale associated with superconductivity (ξ) is larger ($k_F^{-1} \ll \xi$), one should expect to see the effect of electron confinement on superconductivity even when $a \gg k_F$, i.e., for junctions with much higher conductances.

For electrons to undergo an Andreev reflection at the barrier, the energy due to lateral confinement should be such that

$$2\Delta \geq (E_t)_{\min} = (\hbar^2 \pi^2 / 4ma^2). \quad (10)$$

This can be expressed as $ak_F > (\pi/2)(E_F/\Delta)^{1/2}$. For example, in Pb this implies $ak_F \geq |128|$. Using relation (5) we find that this implies $G_0 \simeq 1$ S. Therefore, for junctions with conductance $G_0 \leq 1$ S, the minimum energy for confinement exceeds the energy gap. Under such conditions, the N - S point contact should not show any characteristics of superconductivity and the Andreev reflection peak observed for $|eV| < \Delta$ should begin to disappear for $G_0 \leq 1$ S. From Figs. 5 and 6, we find that for N - S junctions with $G_0 < 1$ S, the manifestation of superconductivity as revealed through the Andreev reflection indeed starts to vanish. If we think of the scale of confinement in terms of a coherence length ξ , then for junctions with $G_0 \simeq 1$ S, $a \simeq \xi/10$. The N - S point contact showing the Andreev reflection is generally analyzed using the BTK model or some of its modifications.^{12,21} The model reproduces some of the observed behavior of N - S point contacts for junctions with high conductance (> 1 S). However, this model has no provision for treating the effect of electron confinement on the properties of the junctions. To be precise, the BTK model has no explicit *length scale* and only one energy scale (the superconducting gap Δ) enters the model through the BCS density of states. We

know of no other model which treats the effect of electron confinement in the context of the Andreev reflection as seen in small N - S point contacts. (There have been recent theories for the effect of confinement and quantization in Josephson currents in small S - S microcontacts.²² These theories mainly treat the pair current through the junction and not the Andreev current. As a result, they are not of much relevance in this context.)

Before conclusion, we would like to mention briefly some interesting reports of $G(V)$ curves in break junctions, point contacts, and STM junctions on high- T_c oxide superconductors (Y-Ba-Cu-O) and Bi-Sr-Ca-Cu-O systems). A decreasing background conductance ($\partial G/\partial V < 0$) has been observed in such junctions.²³⁻²⁵ This is in contrast with the oft-quoted linear normal-state conductance in these systems. Decreasing $G(V)$ within the superconducting energy gap region (typically 20-30 mV) has been associated with the Andreev reflection.^{24,25} In other cases, a well-defined tunneling gaplike feature is seen, above which the normal-state conductance decreases with increasing bias voltage.²³ A variety of interpretations including heating effects and decreasing density of states have been given to account for this behavior. At this point it is difficult to correlate this with our observations presented in this paper as the conductance range where the crossover occurs is very different. Nevertheless, it would be interesting to see whether confinement effects play a role in the junctions made on high- T_c materials as the decreasing $G(V)$ feature has been observed only in break junctions, point contacts, and STM junctions, all of which essentially qualify as "small-area junctions."

To summarize, our observation for both N - N and N - S point contacts shows that electron confinement effects play an important role. We show that, though for $l_e \gg a$ one achieves ballistic contacts with a high Knudsen number, electron confinement effects dominate at still smaller a . At $a \sim k_F^{-1}$ we have most of the junction current coming from evanescent states and the point-contact conductance characteristics resemble that associated with a tunnel junction. The transition from a metallic to tunneling regime has some similarity to the metal-nonmetal transition in solids and the similarity of the criterion $ak_F \simeq 2$ with the Ioffe-Regel criterion is not regarded as fortuitous. We also find that in N - S point contacts, when the junction size $a \ll \xi$, features due to the Andreev reflection disappear. The scenario presented here is a reminder that the quantum effects in small point-contact junctions cannot be neglected. A proper theoretical approach, including consideration of interference of back-scattered electrons near the point contact, is called for in treating these effects.

ACKNOWLEDGMENTS

This work was supported by DAE, Govt. of India as a sponsored scheme and partial equipment support came from JNCASR.

- ¹G. Binnig, H. Rohrer, Ch. Gerber, and E. Weibel, *Phys. Rev. Lett.* **49**, 57 (1982).
- ²J. K. Gimzewski and R. Möller, *Phys. Rev. B* **36**, 1284 (1987), and references therein.
- ³A. G. M. Jansen, A. P. van Gelder, and P. Wyder, *J. Phys. C* **13**, 6073 (1980); A. M. Duif, A. G. M. Jansen, and P. Wyder, *J. Phys.: Condens. Matter* **1**, 3157 (1989).
- ⁴Yu. V. Sharvin, *Zh. Eksp. Teor. Fiz.* **48**, 984 (1965) [*Sov. Phys. JETP* **21**, 655 (1965)].
- ⁵R. Landauer, *IBM J. Res. Dev.* **1**, 223 (1957); Y. Imry, in *Directions in Condensed Matter Physics*, edited by G. Grinstein and G. Mazenko (World Scientific, Singapore, 1986).
- ⁶I. O. Kulik, A. N. Omel'yanchuk, and R. L. Shekhter, *Fiz. Nizk. Temp.* **3**, 1543 (1977) [*Sov. J. Low. Temp. Phys.* **3**, 740 (1977)]; I. O. Kulik and I. K. Yanson, *ibid.* **4**, 1267 (1978) [*ibid.* **4**, 596 (1978)].
- ⁷*Principles of Electron Tunneling Spectroscopy*, edited by E. L. Wolf (Oxford University Press, New York, 1985).
- ⁸D. V. Averin and K. K. Likharev, *J. Low. Temp. Phys.* **62**, 345 (1986); T. A. Fulton and G. J. Dolan, *Phys. Rev. Lett.* **59**, 109 (1987); G. V. Shivashankar and A. K. Raychaudhuri, *Pramana-J. Phys.* **35**, L503 (1990).
- ⁹S. Gregory, *Phys. Rev. B* **44**, 12 868 (1991).
- ¹⁰S. Ciraci and E. Tekman, *Phys. Rev. B* **40**, 11 969 (1989); E. Tekman and S. Ciraci, *ibid.* **43**, 7145 (1991); N. D. Lang, *ibid.* **36**, 8173 (1987).
- ¹¹A. F. Andreev, *Zh. Eksp. Teor. Fiz.* **46**, 1823 (1964) [*Sov. Phys. JETP* **19**, 1228 (1964)].
- ¹²G. E. Blonder, M. Tinkham, and T. M. Klapwijk, *Phys. Rev. B* **25**, 4515 (1982).
- ¹³H. Srikanth and A. K. Raychaudhuri, *Cryogenics* **31**, 421 (1991).
- ¹⁴E. Paulus, Ph.D. thesis, University of Köln, Germany, 1985.
- ¹⁵P. C. van Son, H. van Kempen, and P. Wyder, *J. Phys. F* **18**, 2211 (1988); J. Kirtley, *Int. J. Mod. Phys. B* **4**, 201 (1990), and references therein; H. Srikanth and A. K. Raychaudhuri, *Phys. Rev. B* **45**, 383 (1992).
- ¹⁶G. E. Blonder and M. Tinkham, *Phys. Rev. B* **27**, 112 (1983).
- ¹⁷A. W. Kleinsasser, T. N. Jackson, D. McInturff, F. Rammo, G. D. Pettit, and J. M. Woodall, *Appl. Phys. Lett.* **57**, 1811 (1990).
- ¹⁸R. Kubo, *J. Phys. Soc. Jpn.* **17**, 975 (1962).
- ¹⁹A. F. Ioffe and A. R. Regel, *Prog. Semicond.* **4**, 237 (1960).
- ²⁰B. J. van Wees, H. van Houten, C. W. J. Beenakker, J. G. Williamson, L. P. Kouwenhoven, D. van der Marel, and C. T. Foxon, *Phys. Rev. Lett.* **60**, 848 (1988); A. Szafer and A. D. Stone, *ibid.* **62**, 300 (1989); E. N. Bogachek, A. N. Zagoskin, and I. O. Kulik, *Fiz. Nizk. Temp.* **16**, 1404 (1990) [*Sov. J. Low Temp. Phys.* **16**, 796 (1990)].
- ²¹M. Kupka, *J. Phys: Condens. Matter* **2**, 10 599 (1990); H. Srikanth and A. K. Raychaudhuri, *Physica C* **190**, 229 (1992).
- ²²H. van Houten, *Appl. Phys. Lett.* **58**, 1326 (1991); C. W. J. Beenakker and H. van Houten, *Phys. Rev. Lett.* **66**, 3056 (1991).
- ²³D. Mandrus, L. Forro, D. Koller, and L. Mihaly, *Nature* **351**, 460 (1991); Q. Huang, J. F. Zasadzinski, K. E. Gray, E. D. Bukowski, and D. M. Ginsberg, *Physica C* **161**, 141 (1989); T. Hasegawa, M. Nantoh, and K. Kitazawa, *Jpn. J. Appl. Phys.* **30**, L276 (1991).
- ²⁴H. Srikanth and A. K. Raychaudhuri, *Phys. Rev. B* **45**, 383 (1992).
- ²⁵K. E. Gray, *Mod. Phys. Lett. B* **2**, 1125 (1988).